

Magnetic and transport properties of the rare-earth-based Heusler phases $RPdZ$ and RPd_2Z ($Z = Sb, Bi$)

K. Gofryk, D. Kaczorowski,* and T. Plackowski

Institute of Low Temperature and Structure Research, Polish Academy of Sciences, P.O. Box 1410, 50-950 Wrocław, Poland

A. Leithe-Jasper and Yu. Grin

Max-Planck-Institut für Chemische Physik fester Stoffe, Nöthnitzer Strasse 40, 01187 Dresden, Germany

(Received 3 February 2005; revised manuscript received 7 June 2005; published 9 September 2005)

Four series of ternary compounds $RPdSb$ ($R=Y, Ho, Er$), $RPdBi$ ($R=Nd, Y, Dy, Ho, Er$), RPd_2Sb ($R=Y, Gd-Er$), and RPd_2Bi ($R=Y, Dy-Er$) were studied by means of magnetization, magnetic susceptibility, electrical resistivity, magnetoresistivity, thermoelectric power, and Hall effect measurements, performed in the temperature range 1.5–300 K and in magnetic fields up to 12 T. All these ternaries, except for diamagnetic Y-based phases, exhibit localized magnetism of R^{3+} ions, and a few of them order antiferromagnetically at low temperatures ($T_N=2-14$ K). The equiatomic compounds show half-metallic conductivity due to the formation of narrow gaps in their electronic band structures near the Fermi energy. Their Seebeck coefficient at room temperature is exceptionally high (S up to $200 \mu V/K$), being promising for thermoelectric applications. In contrast, all the 1:2:1 phases are semimetals and their thermoelectric power is much lower (maximum S of $10-25 \mu V/K$). The Hall effect in the compounds studied corroborates complex character of their electronic structure with multiple electron and hole bands with different temperature and magnetic field variations of carrier concentrations and their mobilities.

DOI: [10.1103/PhysRevB.72.094409](https://doi.org/10.1103/PhysRevB.72.094409)

PACS number(s): 71.20.Eh, 71.55.Ak, 72.15.Eb, 72.15.Jf

I. INTRODUCTION

The phases of the general compositions XYZ and XY_2Z , where X and Y stand for d - or f -electron transition metals and Z denotes a p -electron element, continuously attract much attention due to their remarkable magnetic and electrical transport properties.^{1,2} Equiatomic compounds crystallize with the $MgAgAs$ type of structure (space group $F\bar{4}3m$) and exhibit semimetallic or semiconducting behavior. In systems like $XNiSn$ ($X=Ti, Hf, Zr$) (Refs. 3 and 4) the presence of a vacancies sublattice gives rise to the formation of a narrow gap near the Fermi level of the size of several tenths electron volts. This feature leads to high values of the Seebeck coefficient and thus the XYZ compounds are considered as attractive candidates for thermoelectrical applications.⁵⁻⁸

In turn, the XY_2Z Heusler phases ($AlCu_2Mn$ type, space group $Fm\bar{3}m$) usually show metal like conductivity. Interestingly, within this series of alloys several superconductors have been discovered, e.g., RPd_2Sn ($R=Er, Tm, Yb, Lu, Y, Sc$) (Refs. 9–12) and RPd_2Pb ($R=Tm, Yb, Lu, Y, Sc$).¹³ Most spectacularly, in $ErPd_2Sn$ (Ref. 11) and $YbPd_2Sn$ (Ref. 12) the superconductivity was found to coexist with long-range magnetic ordering.

Isostructural phases $RPdZ$ and RPd_2Z were reported to exist with $Z=Sb$ and Bi (Ref. 14) but, to the best of our knowledge, no data on their physical properties have been published yet, except those for a heavy-fermion compound $YbPd_2Sb$ (Ref. 15) and a short account on the magnetic behavior in $RPdSb$ ($R=Dy, Ho, Er$).^{16,17} Thus, in this paper we report some results of our systematic study on the structural, magnetic, thermal, and electrical transport of the phases $RPdSb$ ($R=Y, Ho, Er$), $RPdBi$ ($R=Nd, Y, Dy, Ho, Er$), RPd_2Sb ($R=Y, Gd-Er$), and RPd_2Bi ($R=Y, Dy-Er$).

II. EXPERIMENTAL DETAILS

Polycrystalline samples of $RPdSb$ ($R=Y, Dy, Ho, Er$), $RPdBi$ ($R=Y, Dy, Ho, Er$), RPd_2Sb ($R=Y, Gd, Tb, Dy, Ho, Er$), and RPd_2Bi ($R=Y, Dy, Ho, Er$) were prepared by arc melting the constituents ($R: 99.9 \text{ wt } \%$, $Pd: 99.999 \text{ wt } \%$, $Sb: 99.999 \text{ wt } \%$, $Bi: 99.999 \text{ wt } \%$) under argon atmosphere. The ingots were then wrapped in tantalum foil, sealed in evacuated quartz tubes, and annealed at temperatures ranging from 800 to 1000 °C for several weeks (in the case of the $REPdBi$ phases such a heat treatment led to multiphase products and therefore as-cast samples were used in physical measurements). Quality of the obtained materials was checked at room temperature by powder x-ray diffraction (Huber Guinier G670 image plate camera with $CuK\alpha_1$ radiation, $\lambda=1.5406 \text{ \AA}$, and silicon as an internal standard, $a=5.43119 \text{ \AA}$), energy dispersive x-ray (EDX) analysis [Philips XL30 scanning electron microscope with an integrated energy dispersive spectrometer system and a super ultra-thin window Si(Li) detector] and optical metallography [Zeiss Axioplan 2 optical microscope with a charge-coupled device (CCD) camera]. The samples were found to be single phase with the expected cubic structures of the $MgAgAs$ or $AlCu_2Mn$ type, and with the lattice parameters close to those given in the literature.^{14,16} For $HoPd_2Bi$ powder x-ray diffraction was extended to temperatures down to 50 K (Siemens D-5000 powder diffractometer with $CuK\alpha_1$ radiation equipped with a helium low-temperature attachment). This study revealed a phase transition from cubic to lower symmetry structure occurring at about 135 K.

Magnetic studies were carried out in the temperature range 1.7–300 K and in magnetic fields up to 5 T using a

TABLE I. Ordering temperatures and Curie-Weiss parameters for $RPdSb$, $RPdBi$, RPd_2Sb , and RPd_2Bi alloys; P: paramagnetic behavior, D: diamagnetic behavior.

Compound	T_N [K]	Θ_p [K]	$\mu_{eff}[\mu_B]$
ErPdSb	P	-4.2	9.43
HoPdSb	2	-9	10.7
DyPdSb	3.3	-11.5	10.5
YPdSb	D		
ErPdBi	P	-4.56	9.2
HoPdBi	2.2	-6.12	10.59
DyPdBi	3.5	-11.92	10.7
GdPdBi	13.5	-36.5	8
YPdBi	D		
ErPd ₂ Sb	P	-2.7	9.4
HoPd ₂ Sb	P	-4.7	10.5
DyPd ₂ Sb	2.2	-6.1	10.4
TbPd ₂ Sb	3.1	-7.9	9.6
GdPd ₂ Sb	5.1	-9.8	7.9
YPd ₂ Sb	D		
ErPd ₂ Bi	P	-5.1	9.58
HoPd ₂ Bi	5.2	-17.9	9.94
DyPd ₂ Bi	6.5	-14.7	10.8
YPd ₂ Bi	D		

superconducting quantum interference device (SQUID) magnetometer (Quantum Design MPMS-5). The electrical resistivity was measured from 4.2 to 300 K by a four-point dc technique. Transverse magnetoresistivity and Hall effect measurements were performed within the temperature range 1.5–300 K and in applied fields up to 12 T (Oxford Instruments TESLATRON). The thermoelectric power was measured from 6 to 300 K employing a differential method with copper as a reference material.

III. MAGNETIC PROPERTIES

All the equiatomic compounds, but diamagnetic YPdSb and YPdBi, were found to exhibit localized magnetism of R^{3+} ions. DyPdSb, HoPdSb, GdPdBi, DyPdBi, and HoPdBi order antiferromagnetically at low temperatures ($T_N = 2.0$ –13.5 K), whereas ErPdSb and ErPdBi remain paramagnetic down to the lowest temperature studied. It is worthwhile noting that the Néel temperature derived here for HoPdSb is slightly lower than that determined before by means of powder neutron diffraction ($T_N = 2.7$ K).¹⁸ In the paramagnetic region the susceptibility of all these compounds exhibits a Curie-Weiss behavior with the effective magnetic moments μ_{eff} close to the theoretical values given by the Hund rules for the respective R^{3+} ions ($=g[J(J+1)]^{1/2}$), and with the paramagnetic Curie temperatures Θ_p being negative, i.e., consistent with antiferromagnetic exchange interactions (see Table I).

The magnetic studies on the compounds RPd_2Sb and RPd_2Bi revealed at low temperatures (2.2–6.5 K) the presence of fairly broad maxima in the magnetic susceptibility of

the Dy-, Tb-, and Gd-based antimonides and for the Ho- and Dy-based bismuthides. These features likely manifest the onsets of antiferromagnetic ordering. However it should be noted that the susceptibility decrease below T_N is quite small, and $\chi(T)$ is irreversible when measured in weak fields in zero-field-cooled (ZFC) and field-cooled (FC) conditions [as a typical example, Fig. 1(a) displays the susceptibility of DyPd₂Sb]. Similar behavior was observed before, e.g., for the RPd_2Pb phases,¹³ and might be attributed to spin glass phenomena due to some structural disorder and/or topological frustration of magnetic interactions in the fcc lattice. Moreover, for TbPd₂Sb and DyPd₂Bi other phase transitions, possibly spin reorientations, were found to take place at $T_1 = 2.4$ and 3 K, respectively [as an example, Fig. 1(b) shows the susceptibility of DyPd₂Bi]. In contrast, ErPd₂Sb, HoPd₂Sb and ErPd₂Bi remain paramagnetic down to 1.7 K, while YPd₂Sb and YPd₂Bi exhibit a weak diamagnetism. In the paramagnetic region the susceptibility of each of the 1:2:1 compounds, except for the alloys with yttrium, follows a Curie-Weiss law with the parameters given in Table I. Like in the $RPdZ$ materials studied, the local magnetic moments are carried here by R^{3+} ions, while negative Θ_p 's imply electronic correlations of antiferromagnetic character.

IV. ELECTRICAL TRANSPORT PROPERTIES

A. Electrical resistivity

The electrical conductivities of the $RPdSb$ and $RPdBi$ compounds exhibit the magnitudes and overall temperature dependencies characteristic of semimetals or narrow-gap semiconductors. As typical examples, there are shown in Fig.

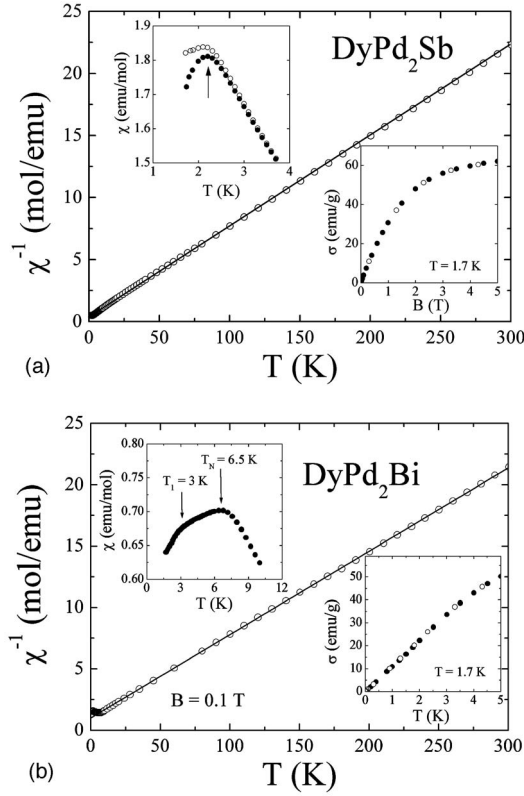


FIG. 1. Reciprocal molar magnetic susceptibility versus temperature for DyPd₂Sb (a) and DyPd₂Bi (b). The solid lines are Curie-Weiss fits. Upper inset in panel (a) shows the low-temperature susceptibility measured in $B=0.01$ T in zero-field-cooled (full circles) and field-cooled (open circles) regimes. The arrow marks the magnetic phase transition. Upper inset in panel (b) shows the low-temperature susceptibility measured in $B=0.1$ T upon cooling the sample in zero field. The arrows mark the two magnetic phase transitions. Lower insets: field dependencies of the magnetization measured at $T=1.7$ K with increasing (full circles) and decreasing (open circles) magnetic field.

2 the $\rho(T)$ curves measured for HoPdSb and DyPdBi. The electrical resistivity for both compounds is of the order of 0.4–10 m Ω cm. With decreasing temperature from 300 K it initially increases, goes through a broad maximum at $T_{max}=70$ and 125 K for HoPdSb for DyPdBi, respectively, and then decreases in a metal like manner at lower temperatures. Moreover, in the case of HoPdSb a rapid drop in $\rho(T)$ is observed below ~ 6 K (see the inset to Fig. 2).

The rise of the resistivity in the region 6 K– T_{max} is reminiscent to the behavior of a doped semiconductor in its impurity range, where due to atomic disorder, defects, or improper stoichiometry some donor or acceptor levels are formed, the presence of which governs the conduction at low temperatures. Above T_{max} the $\rho(T)$ variations have a semiconductor like character and may be approximated by the formula

$$\frac{1}{\rho(T)} = \sigma_0 + \sigma_a \exp\left(\frac{-E_g}{k_B T}\right) \quad (1)$$

that accounts for scattering of the conduction electrons excited over the energy gap E_g . The best fit of Eq. (1) to ex-

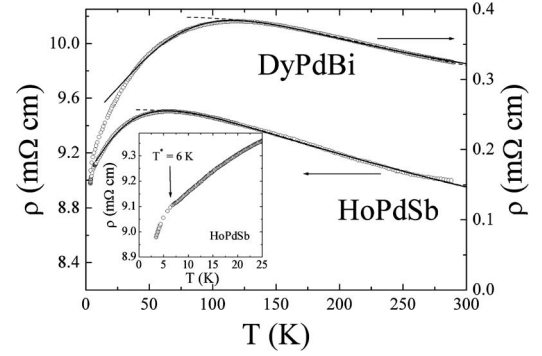


FIG. 2. Electrical resistivity versus temperature for DyPdBi and HoPdSb. The dash and solid lines are least-squares fits of Eqs. (1) and (2), respectively, to the experimental data. Inset: low-temperature resistivity of HoPdSb. The arrow marks the anomaly at $T^*=6$ K.

perimental data yields the following values of the parameters: $\sigma_0=1.1 \times 10^{-4}$ ($\mu\Omega$ cm)⁻¹, $\sigma_a=2.0 \times 10^{-5}$ ($\mu\Omega$ cm)⁻¹, and $E_g=30$ meV in the case of HoPdSb and $\sigma_0=2.6 \times 10^{-3}$ ($\mu\Omega$ cm)⁻¹, $\sigma_a=3.8 \times 10^{-3}$ ($\mu\Omega$ cm)⁻¹, and $E_g=50$ meV for DyPdBi.

The values of E_g derived from the experimental data of HoPdSb and DyPdBi may be compared with those of about 200–500 meV calculated for the alloys XNiSn and XNiSb ($X=Ti, Zr, Hf$).^{19,20} Similarly, the gap calculated for a closely related antimonide LuPdSb is $E_g \sim 100$ meV.²¹ Apparently, the values of E_g obtained for HoPdSb and DyPdBi are considerably smaller than those predicted theoretically and thus most probably the intrinsic regime is not reached in these compounds even at temperatures close to 300 K.

Alternatively, the overall temperature behavior of the electrical resistivity of RPdZ compounds may be described in the framework of a simple model of the electronic band structure in small-gap semiconductors, as formulated in Ref. 22 for a series of skutterudites $ENi_4Sb_{12-x}Sn_x$ ($E=Sn, Eu, Yb$). In this approach one considers two rectangular bands of the height N separated by an energy gap E_g and the Fermi level situated just below the gap. The resistivity of such a system may be expressed as

$$\rho(T) = \frac{n_0 \rho_0 + \rho_{ph}(T)}{n(T)}, \quad (2)$$

where ρ_0 stands for the residual resistivity, n_0 denotes a number of charge carriers at $T=0$ K, $n(T)$ is the temperature-dependent total number of carriers, and $\rho_{ph}(T)$ represents scattering of conduction electrons by phonons, which for temperatures above $\Theta_D/10$ (Θ_D -Debye temperature) can be approximated by the function $\rho_{ph}(T)=AT$. The term $n(T)$ is given by

$$n(T) = \sqrt{n_h(T)n_e(T)} + n_0, \quad (3)$$

where the concentrations of holes $n_h(T)$ and electrons $n_e(T)$ are calculated from general statistical laws

$$n_h(T) = -Nk_B T \ln 2, \quad (4)$$

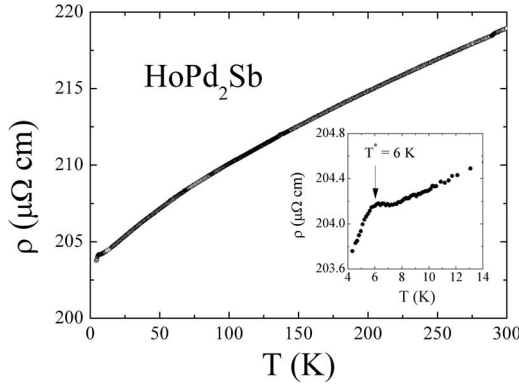


FIG. 3. Electrical resistivity versus temperature for HoPd_2Sb . Inset: low-temperature resistivity. The arrow marks the anomaly at $T^* = 6$ K.

$$n_e(T) = -NE_g + Nk_B T \ln 2 \left[1 + \left(\frac{E_g}{k_B T} \right) \right]. \quad (5)$$

As it seen in Fig. 2, the model proposed provides a quite satisfactory description of the electrical resistivity of HoPdSb and DyPdBi above ~ 25 K. The least-squares fit of Eq. (2) to the experimental data of HoPdSb yields the parameters: $\rho_0 = 9032 \mu\Omega \text{ cm}$, $n_0 = 0.05$ per formula unit, $N = 1.6 \text{ eV}^{-1}$, $A = 0.7 \mu\Omega \text{ cm/K}$, and $E_g = 14 \text{ meV}$. The values of ρ_0 , n_0 , N , A , and E_g derived from the experimental data of DyPdBi are equal to $237 \mu\Omega \text{ cm}$, 0.16 per formula unit, 24.5 eV^{-1} , $0.3 \mu\Omega \text{ cm/K}$, and 35 meV , respectively. It is worth to note that the so-estimated values of the band gap are of the order of those derived in the other approach [Eq. (1)]. Moreover, the number of carriers n_0 as well as the parameter N characterizing the bands nicely reflect the difference between the two compounds studied as regards the character of their electrical conductivity.

In contrast to the RPdZ compounds studied all the RPd_2Sb ternaries exhibit a metal like conductivity (see Fig. 3 for an example). However, the magnitude of the resistivity is relatively large ($200\text{--}300 \mu\Omega \text{ cm}$) and the residual resistivity ratio is quite small ($1\text{--}2$), both findings being probably indicative of considerable atomic disorder. More complex behavior of $\rho(T)$ was found for the RPd_2Bi alloys. At high temperatures the resistivity linearly decreases with decreasing temperatures as expected for simple metals. Then, below a temperature T_{tr} at which a structural phase transition takes place (see Sec. II), the resistivity shows a rapid rise and saturates at low temperatures at values of about $300 \mu\Omega \text{ cm}$. As an example for such behavior Fig. 4 presents $\rho(T)$ measured for HoPd_2Bi . At high temperatures the resistivity of HoPd_2Bi can be well described by the formula $\rho(T) = \rho_0 + AT$ with the parameters: $\rho_0 = 101 \mu\Omega \text{ cm}$ and $A = 0.09 \mu\Omega \text{ cm/K}$. Below the temperature of the structural phase transition the resistivity shows a semiconducting like behavior and may be described by Eq. (1). The values of σ_0 , σ_a , and E_g derived from the experimental data are equal to $\sigma_0 = 3.4 \times 10^{-3} (\mu\Omega \text{ cm})^{-1}$, $\sigma_a = 4.7 \times 10^{-3} (\mu\Omega \text{ cm})^{-1}$, and $E_g = 8.9 \text{ meV}$, respectively. As is apparent from the inset to Fig. 4, in the vicinity of $T_{tr} = 135 \text{ K}$ the resistivity exhibits a distinct hysteresis when measured on heating and cooling,

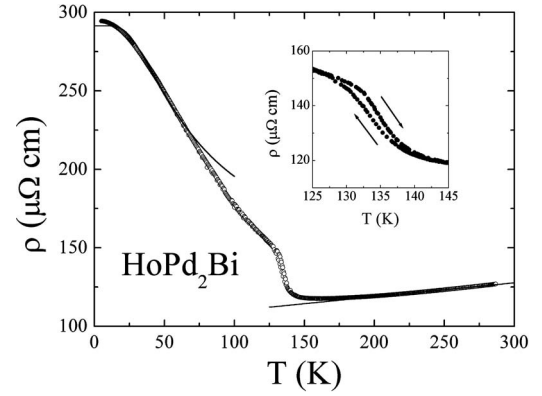


FIG. 4. Electrical resistivity versus temperature for HoPd_2Bi . The solid lines are fits described in the text. Inset: electrical resistivity in the vicinity of the structural phase transition measured with decreasing and increasing temperature (as indicated by the arrows).

which clearly manifests the first-order character of the structural phase transition. The T_{tr} temperatures for the other bis-muthides are as follows: 170 , 168 , and 120 K for Er-, Dy-, and Y-based phases, respectively. It is worthwhile noting that in none of the RPd_2Bi compounds is the transition at T_{tr} accompanied by any anomaly in the magnetic susceptibility.

For the magnetically ordered RPdZ and RPd_2Z compounds one observes some weak anomalies in their $\rho(T)$ that may be associated with the magnetic phase transitions. Moreover, most unexpectedly, the resistivity of all the Er-based phases, HoPdSb and HoPd_2Sb (see Figs. 2 and 3) show below a temperature $T^* = 6\text{--}7 \text{ K}$ a distinct drop that can hardly be attributed to a magnetic phase transition because in this temperature region both the magnetic susceptibility and the specific heat²³ are featureless. This intriguing issue has recently been discussed for the case of the Er-based compounds in Ref. 24 and because of its still unclear nature remains a subject of our on-going research.

B. Seebeck coefficient

Thermoelectric power measurement of RPdSb and RPdBi compounds revealed that the magnitude of the Seebeck coefficient at room temperature is as large as $150\text{--}200 \mu\text{V/K}$ for the antimonides and $40\text{--}80 \mu\text{V/K}$ for the bismuthides. All these materials show positive thermopower in the entire temperature range studied, which indicates that the dominant charge carriers are holes. The overall temperature dependencies of the Seebeck coefficient are similar to those observed before for the alloys XNiSn ($\text{X} = \text{Ti, Hf, Zr}$) (Ref. 25) and characteristic of low carrier density semimetals with parabolic electron and hole bands.²⁶ As examples, in Fig. 5 shown are the $S(T)$ variations for a few compounds. A nearly linear-in- T behavior at high temperatures is probably indicative of diffusion processes. The standard Mott's formula²⁷

$$S(T) = \frac{k_B^2 \pi^2 T}{3eE_F} \quad (6)$$

applied to the experimental data yields the following values of the Fermi energy: $E_F = 32$, 39 , 132 , and 144 meV for

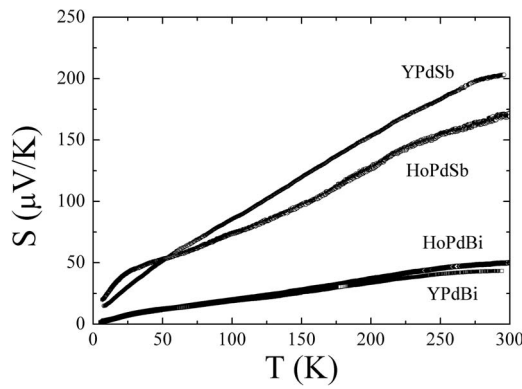


FIG. 5. Thermoelectric power versus temperature for YPdSb, HoPdSb, HoPdBi, and YPdBi.

YPdSb, HoPdSb, HoPdBi, and YPdBi, respectively. These values of E_F are considerably smaller than those characterizing wide-band metals. For HoPdSb a hump below 50 K is observed that presumably comes from phonon drag or/and crystal field effect. The effective carrier concentrations estimated within a single-band model are of the order of 10^{19} cm^{-3} in $RPdSb$ and 10^{20} cm^{-3} in $RPdBi$, being consistent with high magnitude of the electrical resistivity of these compounds.

The Seebeck coefficient is a sensitive probe of electronic band structure near the Fermi level. Its high magnitude is the main prerequisite for efficient thermoelectrical performance, the other factors being moderate electrical resistivity and small heat conductivity. In the case of $ErPdSb$ the two first factors seem fairly appropriate ($S=150 \mu\text{V/K}$ and $\rho=1.8 \text{ m}\Omega \text{ cm}$ at room temperature) and hence measurements of the thermal conductivity $\kappa(T)$ were performed in the temperature range 5–300 K. At room temperature the thermal conductivity is about 3 W/mK (Ref. 28) that leads to a dimensionless figure of merit $ZT=S^2/\rho\kappa$ of about 0.15. The obtained value of ZT is comparable with those typical of 3d-electron transition metal-based XYZ phases, and materials like skutterudites or clathrates, which are being intensively studied in recent years. It is however much lower than the figure of merit achievable for alloys like $\text{Bi}_x\text{Sb}_{2-x}\text{Te}_{3-y}\text{Se}_y$ ($ZT \sim 1$),²⁹ used in state-of-the-art commercial devices.

The thermoelectric power of the RPd_2Z compounds is generally much smaller than that found for the $RPdZ$ alloys. It achieves maximum absolute values of about 4–7 $\mu\text{V/K}$ for the antimonides and 10–25 $\mu\text{V/K}$ for the bismuthides. For all the RPd_2Sb phases the Seebeck coefficient is negative and that of the RPd_2Bi compounds is positive. These findings, together with complex temperature dependencies of the thermopower in both series, clearly indicate the semimetallic character of the compounds with multiple bands of electrons and holes. As an example Fig. 6 presents the $S(T)$ variations for $HoPd_2Sb$ and $ErPd_2Bi$. For both ternaries the thermopower is weakly temperature dependent just below room temperature. Below 170 K, $S(T)$ of the antimonide shows a smooth curved variation toward zero, while that of $ErPd_2Bi$ rapidly increases at the structural phase transition and forms a broad maximum near 110 K. Interestingly, the overall temperature dependence of the thermopower of $ErPd_2Bi$ is very

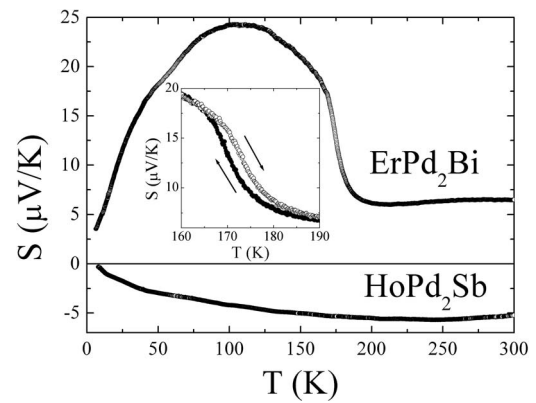


FIG. 6. Thermoelectric power versus temperature for $HoPd_2Sb$ and $ErPd_2Bi$. Inset: thermoelectric power in the vicinity of the structural phase transition in $ErPd_2Bi$, measured with decreasing and increasing temperatures (as indicated by the arrows).

similar to that of its electrical resistivity. In particular, around $T_{tr}=170 \text{ K}$, $S(T)$ shows a pronounced hysteresis (see Fig. 6) closely resembling that observed in $\rho(T)$.

C. Hall effect

The Hall-effect measurements were performed for the Er-based phases only. For all the compounds the Hall coefficient measured in a field of 12 T is positive (see an example in Fig. 7), including the case of $ErPd_2Sb$ that shows negative thermopower. Unlike in metals, R_H is strongly temperature dependent, which implies complex underlying electronic structure with electron and hole bands containing carriers with different temperature-dependent mobilities. Moreover, $R_H(T)$ shows a distinct magnetic field dependence at low temperatures, and the magnitude of the Hall coefficient is reduced with rising field. For $ErPd_2Sb$ one observes a change in the sign of R_H to negative at low temperatures when the Hall effect is measured in weak fields. Such a behavior of R_H clearly manifests a multicarrier nature of the compound studied.

At room temperature the magnitude of R_H is about $10^{-7} \text{ m}^3/\text{C}$ for $ErPdZ$ compounds, $10^{-9} \text{ m}^3/\text{C}$ for $ErPd_2Bi$, and $10^{-10} \text{ m}^3/\text{C}$ for $ErPd_2Sb$. These values are 10^2 – 10^4

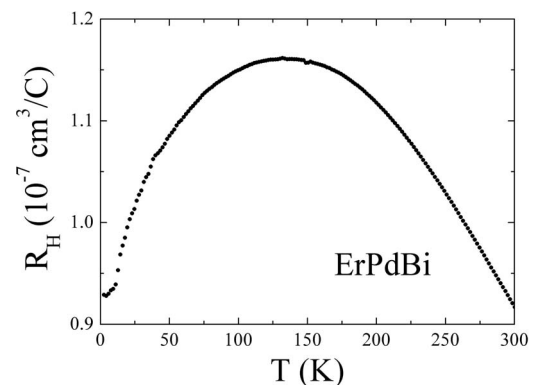


FIG. 7. Hall coefficient versus temperature for $ErPdBi$, measured in a magnetic field of 12 T.

times larger than the Hall coefficient of conventional metals, and 10^2 – 10^3 times larger than that observed for heavy-fermion compounds³⁰ yet typical of semimetallic materials.³¹ Considering a simple single-band model (i.e., assuming as the first approximation that one type of carrier dominates the transport in the multiband systems being discussed), the Hall carrier density is estimated to be of the order of 10^{19} cm⁻³ in ErPdSb and 10^{20} cm⁻³ in ErPdBi, in good agreement with the values obtained from the thermoelectric data. In turn, the Heusler alloys ErPd₂Sb and ErPd₂Bi exhibit much higher carrier density, of the order of 10^{23} and 10^{21} cm⁻³, respectively, in line with the metal like character of their electrical conductivity.

V. SUMMARY

Magnetic susceptibility measurements of the Heusler phases *RPdZ* and *RPd₂Z* ($R=Y, Gd-Er; Z=Sb, Bi$) have revealed that at low temperatures the compounds studied are either paramagnetic or antiferromagnetic with the Néel points of several kelvin. For all these compounds, excluding Y-based alloys, the experimental values of the effective magnetic moment are close to the theoretical ones for respective R^{3+} ions.

Electrical resistivity measurements of the half-Heusler phases *RPdZ* ($Z=Sb, Bi$) have indicated their half-metallic or semimetallic character. At low temperatures the resistivity exhibits a metal like behavior, which is probably due to an impurity band possibly overlapping with the conduction band. At high temperatures the electrical conductivities follow the activation law that accounts for gradual ionization of impurity centers. The positive sign of the Seebeck coefficient

could indicate that holes arising from some acceptor centers are dominant carriers. The energy gaps near the Fermi level are of the order of tens of millielectron volts and thus are much smaller than values estimated from the electronic structure calculations made for similar compounds.^{19–21} The Seebeck coefficient is quite large, of the order expected for low carrier density semimetals. The thermoelectric figure of merit evaluated for ErPdSb is $Z \sim 0.15$ at room temperature. The magnitude of the Hall coefficient is characteristic of semimetals with the carrier densities of the order of 10^{19} – 10^{20} cm⁻³. The sign of R_H is positive, i.e., consistent with the positive sign of S , and conclusively demonstrating that holes dominate in the electronic transport in the *RPdZ* compounds.

While half-Heusler alloys have been characterized as narrow-gap semiconductors all the *RPd₂Sb* and *RPd₂Bi* ternaries have been found to exhibit metal like conductivity. For the *RPd₂Bi* series a structural transformation from cubic to lower symmetry structures is observed that manifests itself as distinct anomalies in the transport characteristics, while no corresponding singularities are observed at the transition temperature in the magnetic data. The thermoelectric power for these materials is much lower than that of the *RPdZ* alloys, being consistent with relatively high values of the carrier densities obtained from the Hall effect measurements.

ACKNOWLEDGMENTS

This work was supported by the Polish State Committee for Scientific Research [Grant Nos. 1 P03B 090 27 (K.G.) and 4 T08A 045 24 (D.K.)]. K.G. and D.K. are grateful to the Max-Planck-Society for supporting their research visits in the MPI-CPFS in Dresden.

*Corresponding author.

- ¹P. J. Webster and K. R. A. Ziebeck, *J. Phys. Chem. Solids* **34**, 1647 (1973).
- ²J. Pierre, R. V. Skolozdra, J. Tobola, C. Hordequin, M. A. Kouacou, I. Karla, R. Currat, and E. Lelievre-Berna, *J. Alloys Compd.* **262–263**, 101 (1997).
- ³R. A. de Groot, F. M. Mueller, P. G. van Engen, and K. H. J. Bushow, *Phys. Rev. Lett.* **50**, 2024 (1983).
- ⁴F. G. Aliev, N. B. Brandt, V. V. Moshchalkov, V. V. Kozyrkov, R. V. Skolozdra, and A. I. Belogorokhov, *Z. Phys. B: Condens. Matter* **75**, 167 (1989).
- ⁵F. G. Aliev, V. V. Kozyrkov, V. V. Moshchalkov, R. V. Skolozdra, and K. Durczewski, *Z. Phys. B: Condens. Matter* **80**, 353 (1990).
- ⁶Y. Xia, S. Bhattacharya, V. Ponnambalam, A. L. Pope, S. J. Poon, and T. M. Tritt, *J. Appl. Phys.* **88**, 1952 (2000).
- ⁷B. A. Cook and J. L. Harringa, *J. Mater. Sci.* **34**, 323 (1999).
- ⁸Q. Shen and L. Zhang, *J. Mater. Sci.* **20**, 2197 (2001).
- ⁹M. Ishikawa, J. L. Jorda, and A. Junod, in *Superconductivity in d- and f-Band Metals* (Kernforschungszentrum, Karlsruhe, 1982) p. 141.
- ¹⁰M. J. Johnson and R. N. Shelton, *Solid State Commun.* **52**, 839 (1984).

- ¹¹R. N. Shelton, L. S. Hausermann-Berg, M. J. Johnson, P. Klavins, and H. D. Yang, *Phys. Rev. B* **34**, 199 (1986).
- ¹²H. A. Kierstead, B. D. Dunlap, S. K. Malik, A. M. Umarji, and G. K. Shenoy, *Phys. Rev. B* **32**, 135 (1985).
- ¹³C. L. Seaman, N. R. Dilley, M. C. de Andrade, J. Herrmann, M. B. Maple, and Z. Fisk, *Phys. Rev. B* **53**, 2651 (1996).
- ¹⁴P. Riani, D. Mazzone, G. Zanichchi, R. Marazza, and R. Ferro, *Z. Metallkd.* **86**, 450 (1995).
- ¹⁵D. Kaczorowski, A. Leithe-Jasper, T. Cichorek, K. Tenya, J. Custers, P. Gegenwart, and Yu. Grin, *Acta Phys. Pol. B* **34**, 125 (2003).
- ¹⁶S. K. Malik and D. T. Adroja, *J. Magn. Magn. Mater.* **102**, 42 (1991).
- ¹⁷A. Zygmunt and A. Szytuła, *J. Alloys Compd.* **219**, 185 (1995).
- ¹⁸G. André, F. Bouree, A. Oleś, W. Sikora, S. Baran, and A. Szytuła, *Solid State Commun.* **104**, 531 (1997).
- ¹⁹S. Ögüt, and K. M. Rabe, *Phys. Rev. B* **51**, 10443 (1995).
- ²⁰P. Larson, S. D. Mahanti, S. Sportouch, and M. G. Kanatzidis, *Phys. Rev. B* **59**, 15660 (1999).
- ²¹K. Mastronardi, D. Young, C. C. Wang, P. Khalifah, R. J. Cava, and A. P. Ramirez, *Appl. Phys. Lett.* **74**, 141 (1999).
- ²²St. Berger, Ph.D. thesis, TU Wien, 2003.
- ²³K. Gofryk, D. Kaczorowski, W. Schnelle, M. Wołczyrz, T. Plack-

- owski, A. J. Zaleski, A. Leithe-Jasper, and Yu. Grin (unpublished).
- ²⁴D. Kaczorowski, K. Gofryk, T. Plackowski, A. Leithe-Jasper, and Yu. Grin, *J. Magn. Magn. Mater.* **290–291**, 573 (2005).
- ²⁵C. Uher, J. Yang, S. Hu, D. T. Morelli, and G. P. Meisner, *Phys. Rev. B* **59**, 8615 (1999).
- ²⁶K. Durczewski and M. Ausloos, *Z. Phys. B: Condens. Matter* **85**, 59 (1991).
- ²⁷R. D. Bernard, *Thermoelectricity in Metals and Alloys* (Taylor and Francis LTD, London 1972).
- ²⁸J. Mucha (private communication).
- ²⁹R. Venkatasubramanian, E. Siivola, T. Colpitts, and B. O'Quinn, *Nature (London)* **413**, 597 (2001).
- ³⁰A. Fert and P. M. Levy, *Phys. Rev. B* **36**, 1907 (1987).
- ³¹F. G. Aliev, *Physica B* **171**, 199 (1991).